RSC Advances

ROYAL SOCIETY OF CHEMISTRY

www.rsc.org/advances

RSC Advances

ARTICLE

Innovative enhancement on gas barrier property of biodegradable poly (butylene succinate) nanocomposite films by introducing confined crystals

Sheng-Yang Zhou[a], Jing-Bin Chen[a], Xu-Juan Li[a], Xu Ji[b], Gan-Ji Zhong[a,*] and Zhong-Ming Li[a,*]

Received 00th January 20xx,
Accepted 00th January 20xx

DOI: 10.1039/x0xx00000x

www.rsc.org/advances

In this work, we creatively obtain high gas barrier poly(butylene succinate) (PBS)/clay nanocomposite films by introducing confined crystals taking advantage of spatial confinement effect which commonly exists in polymer/nanofiller systems. It is found that when the content of clay exceeds a certain amount, the clay can induce some confined crystals around it under the action of spatial confinement effect. These confined crystals and clay would reconstitute into a kind of new "barrier wall" with higher aspect ratio and preferable regularity. As a result, the loss of gas barrier ability caused by crystallinity reduction of PBS and exfoliation degree reduction of clays is effectively compensated. This study provides a newly potential approach to improve the gas barrier property of polymers.

1. Introduction

The demand for biodegradable polymeric film with high gas barrier is rapidly increasing in food packaging industry and agricultural planting.[1-5] As one of the most promising biodegradable polymers, PBS possesses good melt processability and outstanding ductility, showing huge potential in large-scale applications.[6-9] Nevertheless, for various gas-sensitive commodities, the deficient gas barrier performance of PBS film can hardly meet the requirement. Enhancing these poor properties would be a challenge.[10-12]

In the past decade, clay has continually received significant attention for its ability to impart gas barrier to polymers.[13-16] The impermeable clay layers are usually recognized as "nanobarrier walls", making the diffusing gas molecules follow longer and more tortuous permeation pathways to pass through the polymer. Accordingly, the diffusion parameter is significantly decreased.[17-20] Conventional polymer/clay composites obtained via melt mixing generally exhibit only modest improvement in their gas barrier property because of insufficient exfoliation and alignment within the organic polymer matrix.[21-24] To prevent aggregation, the clay concentration rarely exceeds 10 vol. % in traditional polymer/clay composites. Numerous attempts have been made to improve clay exfoliation in polymer matrices, but the improvement in the gas barrier property is still limited by insufficient clay alignment. As a matter of fact, with regard to most semicrystalline polymers, we can also synergistically regulate and control the disperse state of clay and crystal morphology of polymer matrix to achieve desirable performance.[25-26] Unfortunately, the relevant research of the simultaneous influence of clay and crystals on the gas barrier property is still in its infancy, especially when the content of clay is considerably high that is sometime fairly necessary.

In our previous work,[27] we studied the crystallization behavior of PBS in the presence of different content of clay. The result reveals that the growth of PBS crystals was significantly improved compared to that of neat one due to a template effect of clays on PBS crystal growth. But the bulk crystallization kinetics of PBS matrix was suppressed at high clay loadings under the action of spatial confinement effect. It naturally encourages us to investigate those two influences with high clay content on the gas permeation in PBS/clay nanocomposite films. Here we successfully obtain superior gas barrier composite films with high content of clay, meanwhile uncovering the positive function of confined crystals of PBS induced by spatial confinement effect.

2. Experimental

2.1. Materials

PBS, Model bionolle#1001MD, is a commercial product of Showa Denko (Japan), which has a weight-average molecular weight and number-average molecular weight of 2.2 $\times 10^5$ g/mol and 1.1 $\times 10^5$ g/mol, respectively, and a melt flow rate of 1.6 g/10 min (190^{o}C, 2.16 kg). The organically modified clays (I.34TCN), which contain 30-32 wt. % organic modifier, were provided by Amcol International Corporation. The chemical structure of the specific organic modifier of the clays is $CH_3(CH_2)_{17}N(CH_3)[(CH_2CH_2OH)_2]^+$.

[a] College of Polymer Science and Engineering and State Key Laboratory of Polymer Materials Engineering, Sichuan University, Chengdu 610065,P. R. China. E-mails: ganji.zhong@scu.edu.cn (GJZ); zmli@scu.edu.cn (ZML)
[b] College of Chemical Engineering, Sichuan University, Chengdu 610065, P. R. China.

2.2. Preparation of PBS/clay nanocomposite films

Prior to melt compounding, PBS was dried at 80 °C under vacuum for 24 h and the clays were dried at 80 °C under vacuum for 10 h. The melt blending of PBS with clays was performed on a torque rheometer (XSS-300). The compounding was carried out for 10 min at 150 °C with the rotational speed of 50 rpm. Then, all the samples were compression-molded into disc-like films with a thickness of about 250 μm and a diameter of 100 mm at 150 °C under 10 MPa for following characterizations. The weight content of clay in the composites is 0, 1, 5, 10, 20, and 40 wt. %, respectively. For convenience to calculate, the weight content was transformed to volume content (vol. %) by:

$$v = \frac{w\rho_p}{w\rho_p + (1-w)\rho_c} \quad (1)$$

where v and w represents volume content and weight content of clays, respectively. ρ_p and ρ_c are the density of PBS matrix and clay, which are taken as 1.26 g/cm^{3}and 1.8 g/cm^3, respectively. Then, the volume content of clays filled into the PBS matrix can be considered as 0, 0.67, 3.4, 6.9, 14 and 31vol. % according to Equation (1).

2.3. Characterizations

2.3.1. Transmission electronic microscopy (TEM).

The morphology of the as-prepared PBS/clay nanocomposite films were characterized by transmission electronic microscopy with an acceleration voltage of 200 kV (FEI Tecnai F20). Thin sections of the PBS/clay nanocomposite films with a thickness of about 80 nm for TEM observations were prepared by using a Leica EMUC6/FC6 microtome at -100 °C.

2.3.2. Wide-angle X-ray diffraction Testing

PBS crystal in the nanocomposite films was characterized by wide-angle x-ray diffraction, which was carried out at the beamline BC16B of Shanghai Synchrotron Radiation Facility (SSRF, Shanghai, China) with an X-ray detector (Model Mar165). Linear 1D-WAXD profiles were obtained from circularly integrated intensities of the 2D-WAXDpatterns.The crystallinity (X_c) of PBS crystals in the nanocomposite films was calculated by:

$$X_c = \frac{\sum A_{cryst}}{\sum A_{cryst} + \sum A_{amorp}} \quad (2)$$

where A_{cryst} and A_{amorp} represents the fitted areas of crystalline and amorphous phases of PBS, respectively.

2.3.2. Differential scanning calorimetry (DSC)

DSC measurements were performed on a TA DSC Q2000 instrument. About 5 mg of each sample was heated from 40 °C to 150°C at a heating rate of 10 °C/min in a nitrogen atmosphere.

2.3.3. Dynamic mechanical analysis (DMA)

The dynamic mechanical properties of neat PBS and various PBS/clay nanocomposite films were measured with a rheometer RDAII (Scientific, Piscataway, NJ, USA) dynamic analyzer in the tension-torsion mode. The instrument was programmed to measure storage modulus over the temperature range from -80 to 90°C at 3 °C/min of heating rate. The dimension of the test samples was 25 × 5 × 0.6 mm^3 (length × width × thickness). The 2 Hz of constant frequency was used and the applied strain (0.05 %) was located well within the linear viscoelastic region of the samples.

2.3.4. Gas permeability measurement

The gas permeability of neat PBS and its nanocomposite were conducted using a VAC-V2 film permeability testing machine (Labthink instruments, Jinan, China) at room temperature with 50% relative humidity according to ISO2556: 1974.The gas permeation cell was separated into two compartments by film specimen with 100 mm in diameter and about 250 μm in thickness. Air in both compartments was continuously evacuated for 12h prior to testing, ensuring that the pressure changes due to the gas diffusion were greater than the static vacuum pressure changes in the downstream compartment. Subsequently, the gases were discharge into the upstream compartment at a pressure of about 1.01×105 Pa. The pressure changes in the downstream compartment were recorded as a function of time by pressure sensors. The permeability coefficient is determined by the slope of the steady-state permeating line.

3. Results and discussion

3.1. Gas barrier properties of PBS/clay nanocomposite films with wide range of loadings

For gas barrier properties, outstanding gas barrier property of clay is adequately reflected by decreasing gas permeability coefficient of PBS/clay nanocomposite films. Fig.1 reveals the oxygen gas permeability coefficient (P_{O2}) of the neat PBS and PBS/clay nanocomposite films. It can be clearly seen that P_{O2} are effectively reduced with the addition of clay. However, the tendency of permeability decline along with the clay content is obviously divided into two disparate regions. To be specific, with lower content of clay, a 45 % reduction in P_{O2} is obtained from 5.94 × 10^{-15} cm^3 cm cm^{-2} S^{-1} Pa^{-1} in pure PBS film to 3.66 ×10^{-15} cm^3 cm cm^{-2} S^{-1} Pa^{-1} in composite films with 6.9 vol. % clay which manifests a relatively

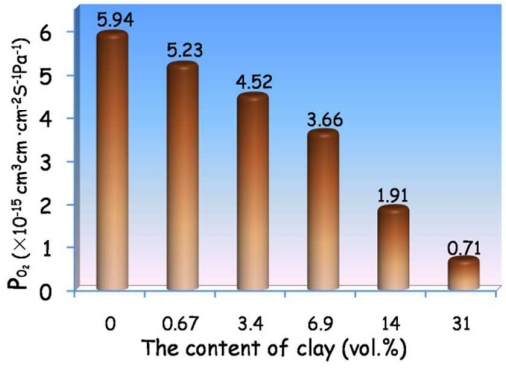

Fig.1 Gas permeability coefficient of PBS/clay nanocomposite films as function of clay content.

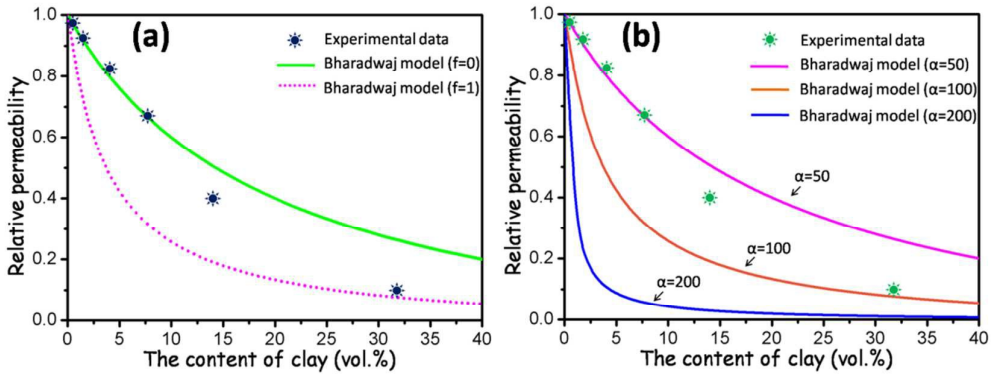

Fig.2 Comparison between experimental data and Bharadwaj model for the relative permeability in terms of clay loadings. (a) Comparison with Bharadwaj model with different value of f defined α=50; (b) Comparison with Bharadwaj model with different value of α defined f=0.

slower decline. While with clay content higher than 14 vol. %, an almost 65% reduction from 1.91×10^{-15} cm^3 cm cm^{-2} S^{-1} Pa^{-1} to 0.71×10^{-15} cm^3 cm cm^{-2} S^{-1} Pa^{-1} in composite films with 32 vol.%, the rate of the decrease is much faster.

We compared our data on O_2 permeability with Bharadwaj model:[28]

$$R_p = \frac{1-\varphi}{1+\varphi(\alpha/2)(2/3)(f+0.5)} \quad (3)$$

Where φ is the volume content of clays and α is the aspect ratio of clay, which was estimated to be about 50 by TEM image of the PBS/clay nanocomposite film containing 0.67 vol. % of clays. $f = 0$ stands for the randomly dispersed morphology of clays in polymer matrix, while $f = 1$ is indicative of the well-ordered oriented array of clays through the entire polymer matrix. The relative permeability (R_p) is estimated as follows:

$$R_p = \frac{P_{c-Gas}}{P_{m-Gas}} \quad (4)$$

where $P_{c\text{-}Gas}$ and $P_{m\text{-}Gas}$ are gas permeability coefficient of PBS/clay nanocomposite films and neat PBS, respectively.

The comparison between experimental data and Bharadwaj model for R_p as a function of clay contents is summarized in Fig.2. As shown in Fig. 2(a), the experimental data of R_P fit well with the line predicted by Bharadwaj model with $f = 0$ as the clay content is lower than 14 vol. %. However, the data obviously locate below these of the predicted Bharadwaj values with $f = 0$, and fit well with the line of $f = 1$ at the clay content of 14 vol. % or 31 vol. %, which is quite unexpected. Besides, the aspect ratio also affects the permeability, Fig. 2(b) exhibits the comparison between experimental data and Bharadwaj model with different value of α. At low clay volume fractions, the data are close to the Bharadwaj curve with α=50, however, at high volume fractions, the data approaches the curve with α= 100. The aforementioned difference can be explained by the following: (1) Bharadwaj model assumes no interaction between the polymer matrix and clay. Some literatures, however, indicated that clay incorporated into the polymer matrix rigidify the polymer chains and inhibit their mobility, in turn imposing restrictions on the free dispersion of clay, resulting in lower free volume and further decrease in permeability. (2) Bharadwaj model disregards the presence of crystals in nanocomposite films, but it is undoubted that a hybrid PBS/clay nanocomposite contains some specific PBS crystals that fill in the spaces between clays.

3.2. Structures of PBS/clay nanocomposite film

TEM observation for PBS/clay nanocomposite films was carried out to assess the dispersion morphology of clays in PBS matrix. Fig.3 presents the typical TEM micrographs of nanocomposite films containing 0.67, 3.4 and 14 vol. % clays respectively. Primarily, one can clearly see that the degree of clay exfoliation decreases gradually with the increase of clay content. When adding only 0.67 vol. % clays into PBS matrix, the majority of clays disperse in the form of individual platelets, suggesting quite good exfoliation. However, as the clay content rises to 3.4 vol. %, hybrid structures are observed which consist of intercalation and exfoliation, and the proportion of completely exfoliated clays is inferior to that of PBS nanocomposite with 0.67 vol. % clay. Further increasing the clay loading to 14 vol. %, the clays mainly show intercalation structure. In order to the better illustration of clay dispersion in PBS, the WAXD patterns at small diffraction angles are given in supplementary information (see Fig. S1). This dependence of clay exfoliation on filler content was also observed in other work.[29-30] With the formation of intercalation structure, more PBS chains are limited into the nanolayer of clays where the interlayer spacing is only about 2.8 nm. Undoubtedly, spatial confinement effect is expected to establish in the nanocomposite films with high clay loadings.

The crystal structure and crystalline morphology of PBS/clay nanocomposite films are explored by 1D-WAXD measurements in

RSC Advances

ARTICLE

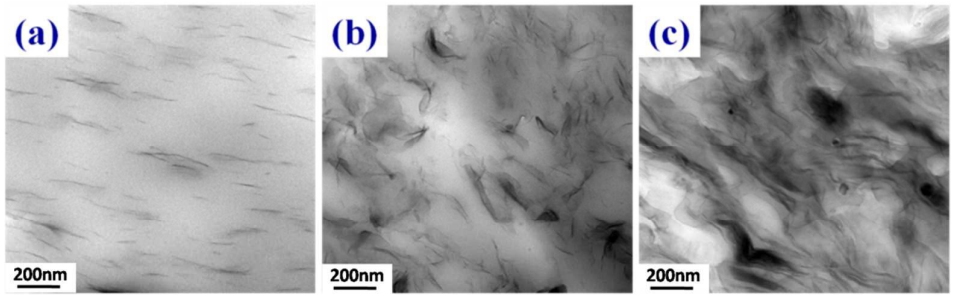

Fig.3 TEM images of the PBS/clay nanocomposite films containing different contents of clays.(a) 0.67 vol. %, (b) 3.4 vol. % and (c) 14 vol. %.

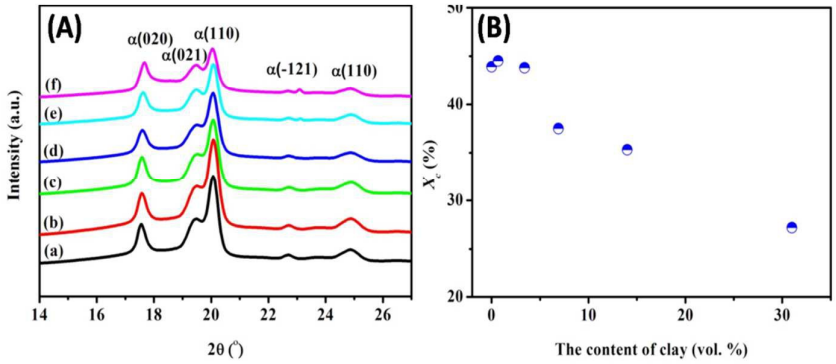

Fig.4 (A) Representative 1D-WAXD curves of (a) neat PBS, PBS nanocomposite films with clay contents of (b) 0.67 vol. %, (c) 3.4 vol. %, (d) 6.9 vol. %, (e) 14 vol. %, and (f) 31 vol. %. (B) The degree of crystallinity of PBS/clay nanocomposite films with different clay contents.

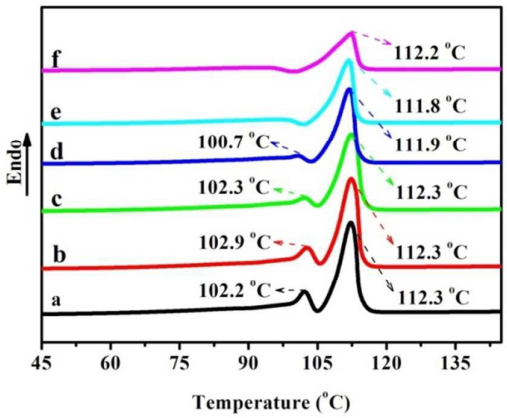

Fig.5 The melting behavior of (a) neat PBS, PBS nanocomposite films with clay contents of (b)0.67 vol. %, (c) 3.4 vol. %, (d) 6.9 vol. %, (e) 14 vol. %, and (f) 31 vol. %.

Table 1 T_{m1}, T_{m2} of PBS/clay nanocomposite films obtained from melting curves.

The content of clay	T_{m1} (°C)	T_{m2} (°C)
Neat PBS	102.2	112.3
0.67 vol. %	102.9	112.3
3.4 vol. %	102.3	112.3
6.9 vol. %	100.7	111.9
14 vol. %	-----	111.8
31 vol. %	-----	112.2

order to obtain more insights into the influences of clays on PBS crystallization. Fig. 4(A) illustrates the 1D-WAXD curves of neat PBS and its nanocomposite films. All the samples show diffraction peak of the α-crystals of PBS with the strong peak intensity at 15.7° and 18.1° representing (020) and (110) reflections, suggesting clays have no impact on the crystalline modification of PBS. Fig. 4(B) gathers the degree of crystallinity (X_c) of PBS/clay nanocomposite films based on the 1D-WAXD curves. The X_c value of PBS nanocomposite films keeps almost invariable at the clay contents below than 6.9 vol. %; however, it decreases obviously at higher

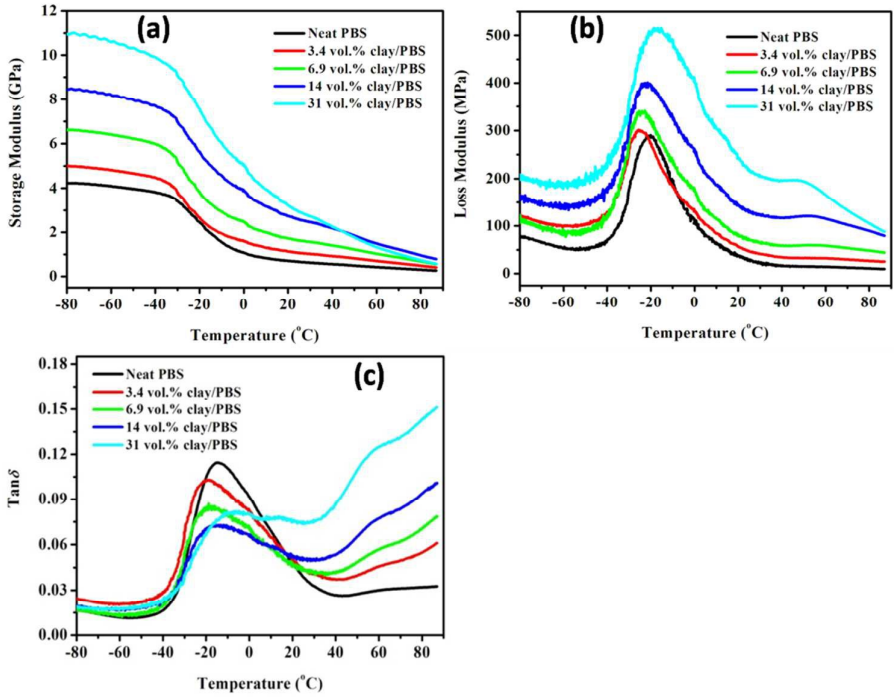

Fig.6 Temperature dependence of (a) storage modulus (E'), (b) loss modulus (E''), and (C) damping parameter (tanδ) for pure PBS and PBS/clay nanocomposite films.

clay contents, the X_c of PBS/clay nanocomposite containing 31 vol. % of clays is only 29.4%, revealing a 36% reduction compared to that of neat PBS. It can be explained by the space restriction of clays, which confines the crystallization of PBS in accordance with the conclusion of our previous works. Moreover, according to our previous results, the crystallization rate of PBS measured by either non-isothermal crystallization or isothermal crystallization is confined by high loadings of clays. The decreased X_c and crystallization rate indicates that a high loading of clays confines the crystal growth of PBS, which once again suggests the formation of spatially confinement environment.[31-32] We further analyzed the PBS/clay nanocomposite film structure by determining its crystallinity with the use of DSC. Fig.5 illustrates the thermograph of PBS and its nanocomposite films during melting at a heating rate of 10 °C/min. From these curves, the melting temperatures are summarized in Table 1. Neat PBS shows double melting peaks, which is ascribed to the re-crystallization and melting mechanism. The low melting point (T_{m1}) stands for the melting of imperfect lamellae of PBS, and the high melting point (T_{m2}) reflects the melting of pre-existed PBS perfect lamellae and re-crystallized lamellae. As the clay content increases from 0.67 up to 31 vol. %, T_{m1} first remains at around 102-103 °C at low clay contents (below 6.9 vol. %), then decreases to 100.7 °C at the clay contents of 6.9 vol. %, and finally disappears at high clay contents (high than 6.9 vol. %). This suggests that the spatial confinement caused by dense clay layers is adverse to the stabilization of PBS imperfect lamellae, resulting in more imperfect lamellae. This result fully indicates that when the content of clay exceeds a certain amount, it could remarkably transform the crystallization habit of PBS. In other words, clay can firstly imposes restriction on the mobility of PBS molecular chain, inducing the crystallization of PBS around its vicinity, thus, the newly formed PBS crystals simultaneously produce continuous barrier layers.

DMA was performed to acquire information on chain motion of PBS and its nanocomposite films. Fig.3 shows the temperature dependence of the storage modulus, loss modulus and tan δ of PBS/clay nanocomposite films at various clay loadings over the temperature range from -80 to 90 °C. Over the entire temperature range, the storage modulus of the nanocomposite films is invariably increased with clay content. For example, at 20 °C, even though the X_c of PBS is evidently decreased, about 350 % increase in storage modulus from 0.71 to 3.2 GPa appears upon addition of 31 vol. % clays. It can be seen from Fig. 3 that tanδ peak (corresponding to T_g) shifts to lower temperature at first, and then turn back to high temperature with the increase of clay content. This means segmental motions are somewhat facilitated in the present of relatively low clay content, which may be attributed to that the modifier of clay accelerates the motion of PBS chain segment; however, segmental motions are restricted with the addition of high loadings of clays, which may be attributed to the strong confinement of clays. Moreover, with increasing addition of clays, tanδ rises more obviously on the heating above T_g, which could be attributed to the relaxation of PBS chains intercalating into clays. Therefore, DMA results certainly verify a spatial confinement effect on molecular mobility of PBS in PBS/clay nanocomposite films, especially at high loadings.

RSC Advances

ARTICLE

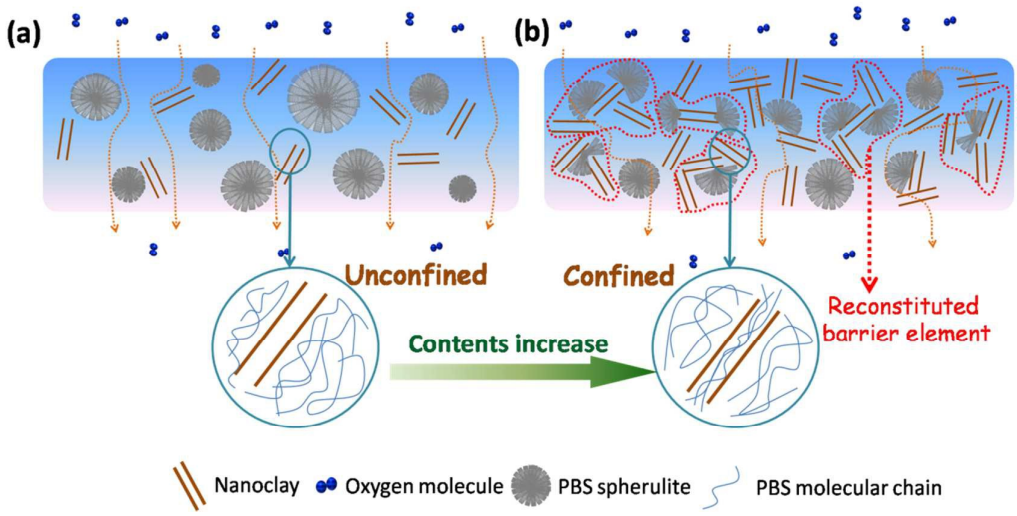

Fig.7 Schematic diagram of possible gas barrier mechanism of PBS/clay nanocomposite films with (a) low content of clay, (b) high content of clay.

3.3 Proposed gas barrier mechanism of PBS/clay nanocomposite films with different contents.

Undoubtedly, "torturous path effect" caused by clays is one of the key factors to improve the gas barrier property of PBS. There are three vital factors that affect the tortuosity of penetration path for diffusing molecules: the volume fraction of the clays, the morphology of clays (exfoliation, dispersion and orientation relative to the diffusion direction), and the aspect ratio of clays. In our study, the exfoliation degree of clays decreases with clay content, and the X_c of PBS is obviously reduced by spatial confinement effect of high loadings of clays. Thus, according to the common sense, the experimental data of R_P for the PBS nanocomposite films with clay contents of 14 vol. % and 31 vol. % should be higher than, but not lower than these of the predicted Bharadwaj values when f=0. What happens in the PBS/clay nanocomposite films containing high clay loadings that lead to this discrepancy? From the comparison between Bharadwaj model and experimental date, we find that with high content of clay, the value of f tends to be 1, and the aspect ratio α become more and more big. It is reasonable to conclude that the spatial confinement effect of clays is the key factor to influence the crystal morphology of PBS, the confined crystals of PBS and high content of clay constitute towards to be a new barrier element which has greater aspect ratio and has a specific tendency to arrange regularly. We propose schematic diagrams in Fig.7 to reveal the possible gas barrier mechanism. During the gas permeation process in PBS/clay nanocomposite films with low content, the dominating barrier elements is incompact PBS spherulite and random clays, while in films with high content, spatial confinement effect of clay induces some crystals round it, the clays are covered with confined crystals, forming a region of clay/crystal hybrid structure which aspect ratio is observably greater, this kind of new "barrier wall" tends to be more inerratic which is beneficial for the enhancement of barrier properties of film in which the path of gas molecules permeation becomes undoubtedly more tortuous.

Conclusions

The gas barrier property of PBS/clay nanocomposite films is effectively enhanced by introducing confined crystals. As predicted by Bharadwaj model, it implies that when the content of clay exceeds a certain amount, the barrier elements act out greater aspect ratio and more regular dispersion. TEM images show that clays are uniformly dispersed in PBS matrix and reveal a morphology evolution from exfoliation to intercalation with clay content increasement. 1D-WAXD and DSC measurements suggests that high content of clays had a negative effect on the PBS imperfect lamellae and decreasing the X_c of PBS which is an obvious effect of spatial confinement, while it is not observed in the nanocomposite films with low clay loadings. The gas barrier properties of PBS are signally enhanced by clays, and substantial improvements were presented in the nanocomposite films combining high loadings of clays. Thereinto, clay can induce some confined crystals around it with the spatial confinement effect. This confined crystals and clay would reconstitute into a new kind of "barrier wall" with higher aspect ratio and preferable regularity, the loss of gas barrier ability

caused by X_c reduction of PBS and exfoliation degree reduction of clays is effectively compensated. This study provides a new view to fabricate polymers with outstanding gas barrier property.

Acknowledgements

The authors gratefully thank the financial support from the National Natural Science of China (Grant Nos. 51473102, 51273131 and 51473101), the Foundation for Innovative Research Groups of the National Natural Science Foundation of China (Grant No. 51121001), China Postdoctoral Science Foundation (Grant No. 2014T70868) and the Specialized Research Fund for the Doctoral Program of Higher Education (Grant No.20120181120101). Our work was also supported by the Fundamental Research Funds for the Central Universities.

Notes and references

1. J. W. Rhim, H. M. Park and S. Chang, *Prog. Polym. Sci.*, 2013, **38**, 1629-1652.
2. N. Padmal, *J. Macromol. Sci. C*, 1999, **39**,481-505.
3. H. Yu and Y. J.Yao, *RSC Adv.*, 2014, **4**, 59792-59802.
4. S. Sinharay and M. Bousmina, *Prog. Mater. Sci.,* 2005, **50**, 962-1079.
5. J. Sara and Risch, *J. Agr. Food Chem.*, 2009, **57**, 8089-8092.
6. X. Shia and Z. Qiu, *RSC Adv.*, 2015, **5**, 79691-79698.
7. L. F. Liu, J. Y. Yu, L. D. Cheng, X. J. Yang, *Polym. Degrad. Stabil.*, 2009, **94**, 90-94.
8. G. Matteo, A. Negroni, M. Soccio, G. Zanaroli, N. Lotti, . Favaand A. Munaria. *Green Chem.*, 2012, **14**, 2885-2893.
9. C. Labruyère, O. Talon, N. Berezina, E. Khousakounband C. Jérôme, *RSC Adv.*, 2014, **4**, 38643-38648.
10. L. Xie, H. Xu, J. B. Chen, Z. J. Zhang, B. S. Hsiao, G. J. Zhong, J. Chen, Z.M. Li, *ACS Appl. Mater. Inter.* 2015, **7**, 8023–8032.
11. T. Mekonnen, P. Mussone, H. Khalilband and D. Bressler, *J. Mater. Chem. A*, 2013, **1**, 13379-13398.
12. B. Chen, J. R. Evans, H. C. Greenwell, P. Boulet, P. V. Coveney, A. A. Bowdenf and A. Whitingc, *Chem. Soc. Rev.*, 2008, **37**, 568-594.
13. Y. Cui, Kumar, R. K. Balakantha and H. Daniel, *RSC Adv.*, 2015, **5**, 63669-63690.
14. R. S. Sinha and M. Okamoto, *Prog. Polym. Sci.*, 2003, **28**, 1539-1641.
15. C. S. Lu and Y. W. Mai, *Phys. Rev. Lett.*, 2005, **95**, 088303.
16. P. Kiliaris and C. D. Papaspyrides, *Prog. Polym. Sci.*, 2010, **35**, 902-958.
17. M. A. Priolo, D. Gamboa and J. C. Grunlan, *ACS Appl. Mater. Inter.*, 2010, **2**, 312-320.
18. M. A. Priolo, D. Gamboa, K. M. Holder and J. C. Grunlan, *Nano Lett.* 2010, **10**, 4970-4974.
19. M. A. Priolo, K. M Holder, D. Gamboa and J. C. Grunlan, *Langmuir*, 2011, **27**, 12106-12114.
20. G. Choudalakis and A. D. Gotsis, *Eur. Polym. J.*, 2010, **45**, 967-984.
21. S. S. Ray, Okamoto, Kazuaki, P. Maiti and M. Okamotoa, *J.Nanosci. Nanotechno.*, 2002, **2**, 171-176.
22. T. Ebina and F. Mizukami, *Adv. Mater.* 2007, **19**, 2450-2453.
23. C. H. Zhou, Z. F. Shen, L. H. Liu and S. M. Liu, *J. Mater. Chem.*, 2011, **21**, 15132-15153.
24. B. Chen, J. R. Evans, H. C. Greenwell, P. Boulet, P. V. Coveney and A. B. Whiting, *Chem. Soc. Rev.*, 2008, **37**, 568-594.
25. K. Oshihiro and O. Masami, *Polymer*, 2009, **50**, 4718–4726.
26. C. Sébastien, F. Nadège, C. Corinne, D. Eric, S. Jérémie, S. Michel and M. Stéphane, *J. Membr. Sci.*, 2015, **496**, 185–198.
27. J. B. Chen, J. Z. Xu, H. Xu, Z. M. Li, G. J. Zhong and J. Lei, *Chinese J. Polym. Sci.*, 2015, **33**, 576-586.
28. R. K. Bharadwaj, *Macromolecules*, 2001, **34**, 9189-9192.
29. H. Wang, J. K. Keum, A. Hiltner, E. Baer, B. Freeman, A. Rozanski and A. Galeski, *Science*, 2009, **323**, 757-760.
30. Y. Li, A. Kaito and S. Horiuchi, *Macromolecules*, 2004, **37**, 2119-2127.
31. S. S. Ray, K. Okamoto and M. Okamoto, *J. Appl. Poly. Sci.*, 2006, **102**, 777-785.
32. V. Krikorian and D. J. Pochan, *Macromolecules*, 2004, **37**, 6480-6491.